

COMMUNICATION



Cite this: *Chem. Commun.*, 2015, 51, 8292

Received 22nd February 2015,
Accepted 8th April 2015

DOI: 10.1039/c5cc01588j

www.rsc.org/chemcomm

Conversion of a metal–organic framework to N-doped porous carbon incorporating Co and CoO nanoparticles: direct oxidation of alcohols to esters†

Yu-Xiao Zhou, Yu-Zhen Chen, Lina Cao, Junling Lu and Hai-Long Jiang*

A Co-based metal–organic framework, ZIF-67, has been exploited as a self-template to afford N-doped porous carbon incorporating Co NPs with surface-oxidized CoO species, which exhibit excellent catalytic activity, selectivity and magnetic recyclability toward the direct oxidation of alcohols to esters with O₂ as a benign oxidant under mild conditions.

Esterification represents one of the most important and fundamental transformations in organic synthesis, as esters are very important moieties and have broad applications in bulk synthesis, fine chemicals, natural products, and polymers.¹ Esters are traditionally prepared by a two-step synthetic procedure from alcohols, involving the synthesis of the carboxylic acids or activated acid derivatives, and a subsequent reaction with alcohols. As we all know, the multi-step reaction process usually results in the waste of reagents and produces unwanted by-products that are environmentally and economically undesired. Given the wide availability of alcohols, the direct oxidation of alcohols to esters in a single step, avoiding the use of the corresponding acids or acid-derivatives, is green, economic and very attractive. However, the relevant reports for this reaction are limited to precious metal-based catalysts, mostly in homogeneous systems, which are economically unfavorable.² To the best of our knowledge, extremely rare non-precious metal catalysts have been reported for direct oxidative esterification of alcohols thus far.³ Therefore, the development of cost-effective, highly efficient and recyclable heterogeneous catalysts for such transformation under mild conditions is of great interest and pivotal importance.

As a relatively new class of crystalline porous materials, metal–organic frameworks (MOFs) have received growing interest.⁴ Currently, MOFs have been found to have potential applications in many fields, such as gas storage and separation, catalysis, sensing, drug delivery, proton conductivity, etc.^{5–8} Given that metal clusters

and organic linkers are well organized in the framework, MOFs with superb structural tunability offer congenial conditions as precursors for constructing nanostructured metal (oxide)/carbon and their nanocomposites, primarily *via* pyrolysis.⁹ In the solid–solid transformation process, MOFs behave as ideal sacrificial templates and their long-range ordering and porosity can be partially preserved. Although in its infancy, it is highly possible and expected that, upon thermal decomposition of MOF hard templates, the resultant metal (oxide) nanoparticles (NPs), distributing throughout the porous carbonaceous matrix with preserved MOF morphology, could be well accessible and very effective for heterogeneous catalysis.^{10,11}

Herein, a zeolite-type MOF, Co(2-methylimidazole)₂ (ZIF-67),¹² as a hard template, has been thermally converted to Co–CoO@N-doped porous carbon nanocomposites with regular shape, in which crystalline Co NPs with surface-oxidized CoO species are well dispersed throughout the N-doped porous carbon. Remarkably, the nanocomposite exhibits excellent catalytic activity and is magnetically recyclable toward selective and direct oxidation of alcohols to esters with molecular oxygen as an oxidant under mild conditions. It is proposed that the special structure of the catalyst and the synergistic effect between Co and CoO account for the superb catalytic performance. To the best of our knowledge, this is the first MOF-derived catalyst and extremely rare non-precious metal-based heterogeneous catalyst for such reaction to date.

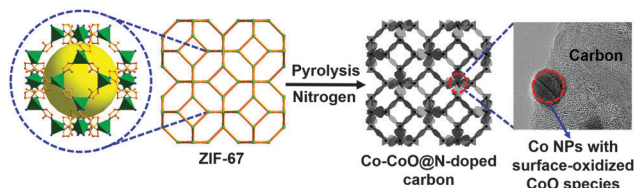
An aqueous solution of Co(NO₃)₂ and 2-methylimidazole being stirred at room-temperature yielded ZIF-67 nanocrystals,¹² which underwent pyrolysis at different temperatures under N₂ to afford Co–CoO@N-doped porous carbon nanocomposites with regular shape (Scheme 1), hereafter denoted as NC-*T-t* (NC, *T* and *t* represent nanocomposite, pyrolysis temperature and time, respectively).

The pure phase of ZIF-67 has been confirmed by powder X-ray diffraction (PXRD) (Fig. S1a, ESI†). Upon thermal treatment at different temperatures, all PXRD patterns show a weak broad peak at ~26° assigned to the typical (002) diffraction of graphitic carbon from the organic moiety and three sharp peaks characteristic of metallic β-Co (Fig. S2 and S3a, ESI†), the intensity of which gradually increases along with elevated annealing temperature, revealing the improved crystallinity of metallic Co and its

Hefei National Laboratory for Physical Sciences at the Microscale, Key Laboratory of Soft Matter Chemistry, Chinese Academy of Sciences, Collaborative Innovation Center of Suzhou Nano Science and Technology, School of Chemistry and Materials Science, University of Science and Technology of China, Hefei, Anhui 230026, P. R. China. E-mail: jianglab@ustc.edu.cn; Fax: +86-551-63607861;

Tel: +86-551-63607861

† Electronic supplementary information (ESI) available. See DOI: 10.1039/c5cc01588j



Scheme 1 Schematic illustration of the synthesis of Co–CoO@N-doped porous carbon nanocomposites via the pyrolysis of ZIF-67.

significant effect with annealing temperature. Raman spectra exhibit two dominant peaks at about 1350 and 1600 cm^{-1} , corresponding to D and G bands, respectively (Fig. S3b, ESI[†]). The intensity of the peaks gradually increases along with elevated annealing temperature, indicating the formation of abundant defects and disordered carbon during the pyrolysis. The contents of Co element are 21.6%, 29%, 32.9% and 39.7%, respectively, for NC-500-3h, NC-600-3h, NC-700-3h and NC-800-3h based on the inductively coupled plasma-atomic emission spectrometry (ICP-AES) data (Table S1, ESI[†]). N_2 sorption measurements show the typical type I isotherms for ZIF-67, matching its microporous character (Fig. S1b, ESI[†]). Upon pyrolysis, all N_2 sorption isotherms are close to type-IV with a hysteresis loop and the NC-700-3h possesses the highest S_{BET} ($291\text{ m}^2\text{ g}^{-1}$) and its pore sizes fall into 1–2.5 nm (Fig. S4, ESI[†]).

The structure and morphology of ZIF-67 and its pyrolysis product NC-700-3h as a representative have been investigated by scanning electron microscopy (SEM) and transmission electron microscopy (TEM) observation. Compared with polyhedral ZIF-67 nanocrystals in 200–500 nm (Fig. S5, ESI[†]), the pyrolysis product NC-700-3h evolves to uniform concave nanocubes with size shrinkage to some extent (~ 150 nm, Fig. 1a). Many NPs of 5–20 nm with high contrast are uniformly distributed in a porous matrix assigned to carbon (Fig. 1b, Fig. S6, ESI[†]). The high-resolution TEM (HRTEM) image unambiguously shows the presence of graphitic layer domains and the crystalline Co with clear lattice spacings of 0.2 nm (Fig. 1c). The selected area electronic diffraction (SAED) pattern further supports the presence of polycrystalline Co (Fig. 1b, inset). The elemental mapping for NC-700-3h demonstrates the co-existence

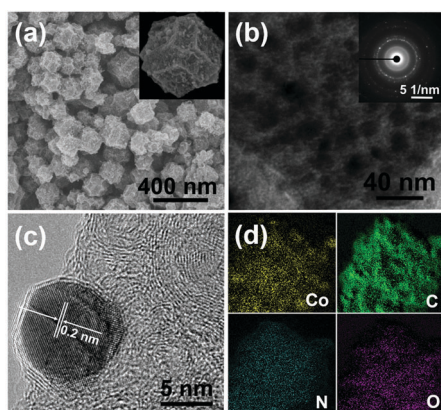


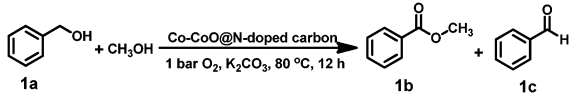
Fig. 1 Microstructure observation for NC-700-3h. (a) SEM image (inset: enlarged particle). (b) TEM image with inset SAED pattern. (c) HRTEM image showing lattice fringes of the crystalline Co NPs and the graphitic layer domains. (d) Elemental mapping showing the uniform dispersion of Co, C, N and a small amount of O elements.

and homogenous dispersion of Co, C, N and a small amount of O species (Fig. 1d), while energy dispersive spectrometry (EDS) analysis verifies that the crystalline particle is composed of Co only and very few O even if present (Fig. S7, ESI[†]). It is assumed that the trace oxygen may be contributed from surface oxidation of cobalt in air,^{9f} which cannot be detected by EDS as a bulk phase characterization tool.

The X-ray photoelectron spectroscopy (XPS) results show that Co, C, N and O are detectable on the surface of NC-700-3h and the Co is composed of Co^0 , Co^{2+} and Co–OH species (Fig. S8, ESI[†]).¹³ In addition, the N 1s spectrum exhibits four distinct peaks with binding energies of 398.8 eV, 399.8 eV, 401.1 eV and 403 eV, which are assignable to pyridinic, pyrrolic, graphitic and oxidized nitrogen, respectively.¹⁴ To gain the structural information in more detail, Ar^+ sputtering has been applied for NC-700-3h. Remarkably, the signals of Co 2p and O 1s exhibit significant changes, where the peak assigned to Co^0 becomes much stronger while the peaks from Co^{2+} and O 1s almost disappear upon 15 s or longer Ar^+ sputtering. The results imply that Co^0 on the external surface is partially oxidized to Co^{2+} while the inner Co^0 well remains in NC-700-3h, which is in agreement with the elemental mapping and EDS results as well as our assumption above. To further understand the existing form of Co species in NC-700-3h, temperature programmed reduction (TPR) has been conducted and it displays the only peak at $\sim 472\text{ }^\circ\text{C}$ (Fig. S9, ESI[†]), which is assigned to the reduction of Co^{2+} ions to metallic cobalt¹⁵ and supports the XPS results above. All these characterizations suggest that the direct pyrolysis of ZIF-67 leads to N-doped porous carbon incorporating well-dispersed crystalline Co NPs, the outer surface of which are partially oxidized to CoO species.

Given that the cobalt with variable chemical valences is able to transfer electrons and act as the active site for oxygen transfer,¹¹ the obtained Co and CoO NPs could be effective in catalytic oxidation. The high-density Co and CoO sites in ZIF-67-derived nanocomposites are uniformly distributed throughout the porous carbon matrix and are well accessible, and the pore structure not only greatly facilitates the transfer of substrates/products but also limits the migration and aggregation of the active NPs, which would render the nanocomposites excellent in catalytic oxidation.

Encouraged by the above considerations, the as-prepared Co–CoO@N-doped carbon nanocomposites were employed for the cross-esterified oxidative reaction between benzyl alcohol and methanol with O_2 as the oxidant and K_2CO_3 as a base (ESI[†] Section S2). As shown in Table 1, NC-700-3h showed the best activity and selectivity to the only targeted product within 12 hours (entry 5). For comparison, the nanocomposites obtained with different pyrolysis temperature and time showed lower activity or/and selectivity to varying extents (entries 1–7). Given that Co_3O_4 NPs were reported to be active for the reaction,^{3a} intuitively we attempted to convert both Co and CoO in NC-700-3h into Co_3O_4 by oxidation at $250\text{ }^\circ\text{C}$ in air for 3 h after calcination at $700\text{ }^\circ\text{C}$ to produce NC-700-3h-250-3h (Fig. S2b, ESI[†]). Unfortunately, the conversion lowered to 48% and the selectivity to methyl benzoate was 56% (entry 8), revealing that Co_3O_4 is not very active in our case. Unexpectedly, both Co/AC and CoO/ SiO_2 offered very low catalytic activity and selectivity (entries 9 and 10). Increasing N contents in the NC-700-3h was found to be even harmful to the conversion (entry 11, ESI[†] Section S2).

Table 1 Methyl esterification of benzyl alcohol and methanol over different Co–CoO@N-doped carbon catalysts^a


Entry	Catalyst	Conversion ^b (%)	Selectivity ^b (%)	
			1b	1c
1	NC-500-3h	51	36	64
2	NC-600-3h	79	73	27
3	NC-700-1 h	71	82	18
4	NC-700-2 h	78	87	13
5	NC-700-3h	100	100	0
6	NC-700-4 h	98	99	1
7	NC-800-3h	95	95	5
8	NC-700-3h-250-3h	48	56	44
9	Co/AC	4	28	72
10	CoO/SiO ₂	0.8	49	51
11	NC-700-3h-N ^c	65	100	0
12 ^d	NC-700-3h	6	4	96
13 ^e	NC-700-3h	40	15	85
14 ^f	NC-700-3h	16	7	93

^a Reaction conditions: 1 mmol benzyl alcohol (1a), 8 mL CH₃OH, 25 mg catalyst, 0.2 mmol K₂CO₃ otherwise mentioned, 1 mmol dodecane was added as an internal standard. ^b Determined by GC or GC-MS. ^c NC-700-3h with increased N contents. ^d Without base and O₂. ^e Without base. ^f Without O₂.

The presence of base and O₂ was demonstrated to be necessary for the conversion (entries 12–14). These results suggest that the special structure of NC-700-3h and the synergistic effect between Co and CoO could play crucial roles in the high catalytic activity and selectivity.

To demonstrate the stability and reusability of NC-700-3h, five more recycles were conducted. As shown in Fig. 2a, both catalytic activity and selectivity remained very well in the six consecutive runs. TEM observation clearly demonstrated the maintained NP size and shape of the catalyst after recycling (Fig. S10, ESI[†]), suggesting its great stability and recyclability. After 6 h of reaction, the catalyst was filtered out and the results showed that no further product was formed even after 24 h under the same conditions (Fig. 2b), inferring that no leaching occurred to the catalyst and the process should be truly heterogeneous. Therefore, the NC-700-3h nanocomposite exhibits superb catalytic activity and selectivity and possesses truly heterogeneous catalytic nature with excellent catalytic stability and recyclability for the esterification reaction. In addition, taking advantage of the strong magnetic properties, the catalyst can be easily separated from the reaction solution and

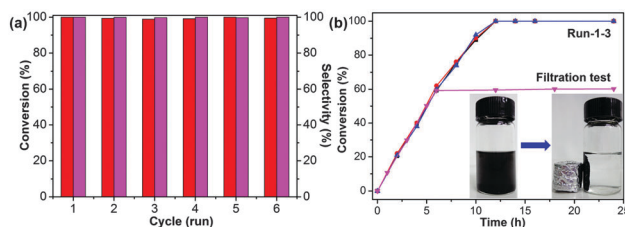


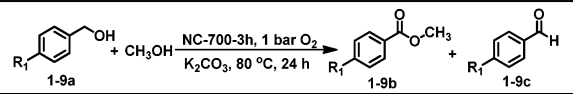
Fig. 2 (a) Conversion and selectivity of six runs of reaction and (b) catalytic recyclability and filtration test of esterification reaction between benzyl alcohol and methanol over NC-700-3h. Inset of (b): the photographs demonstrate the facile separation of the catalyst by a magnet.

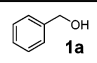
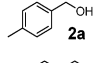
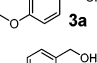
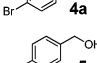
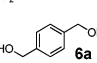
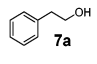
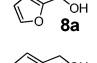
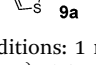
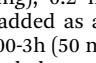
the cloudy suspended solution turns transparent within a few seconds with an external magnet (Fig. 2b, inset).

Upon optimization of reaction conditions with MeOH using benzyl alcohol as a probe substrate, different derivatives of benzylic alcohol have been examined over the NC-700-3h catalyst (Table 2). The reaction of diverse derivatives of benzene methanol in the presence of MeOH afforded the corresponding methyl esters in excellent conversions (entries 2–7). In addition, the oxidative esterification of heterocyclic alcohols with methanol has also been examined, where 2-furanmethanol and 2-thiophenemethanol were obtained with 98% and 85% conversions, respectively (entries 8–9).

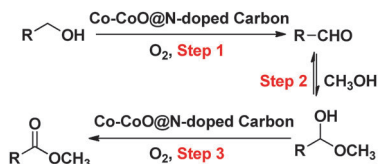
To further demonstrate the general applicability of the NC-700-3h catalyst, diverse benzyl alcohols were investigated in cross-esterification reactions with other aliphatic alcohols (Table S2, ESI[†]). Not surprisingly, all these cross-esterifications for both benzyl and heterocyclic alcohols have shown excellent conversion and selectivity. The benzyl alcohol reacts with other aliphatic alcohols to give their target products in high yields (entries 1–3) and the direct self-esterification of benzyl alcohol also displays high conversion up to 77% and provides only one product (entry 4). Next, the oxidative esterification of both benzyl and heterocyclic alcohols with ethanol has also been investigated. To our delight, ethyl esters of both benzyl and heterocyclic alcohols were obtained in up to 98% conversion (entries 5–12).

Moreover, the oxidative homocoupling reactions with aliphatic alcohols (Table S3, ESI[†]), although seldom studied,^{2c,d} have been

Table 2 Methyl esterification of benzyl alcohol derivatives and methanol over the NC-700-3h catalyst^a


Entry	R ₁	Conversion ^b (%)	Selectivity ^b (%)	
			1d	1e
1		100	100	0
2		98	97.8	2.2
3		100	100	0
4		91	92	8
5		95.6	99	1
6 ^c		100	89	11
7		90	88	12
8		98	90	10
9		85	89	11

^a Reaction conditions: 1 mmol benzyl alcohols (1a–9a), 8 mL CH₃OH, NC-700-3h (25 mg), 0.2 mmol K₂CO₃ otherwise mentioned, 1 mmol dodecane was added as an internal standard. ^b Determined by GC or GC-MS. ^c NC-700-3h (50 mg) and 0.4 mmol K₂CO₃, and the product was dimethyl terephthalate.



Scheme 2 Proposed mechanism for direct oxidative esterification of alcohols over Co–CoO@N-doped porous carbon.

demonstrated to be feasible over the ZIF-67-derived catalyst. In the presence of NC-700-3h, ethanol is able to undergo oxidative esterification and affords ethyl acetate with 54.2% yield under mild conditions (entry 1). Propanol and butanol also exhibit good reactivity to the corresponding aliphatic esters in 57.6% and 59.8% conversions (entries 2–3).

Based on the above results, a possible reaction mechanism for the oxidative esterification of alcohols over Co–CoO@N-doped carbon nanocomposites is illustrated in Scheme 2. The direct synthesis of methyl esters from primary alcohols can be divided to three steps: first of all, alcohols are converted to aldehydes with O_2 as the oxidant and this is considered to be the rate-determining step, probably caused by the abstraction of β -H from alcohols.¹⁶ Secondly, aldehydes and methanol are able to undergo a condensation reaction to give hemiacetal species in the absence of a catalyst, mainly due to the electrophilic properties of aldehydes and nucleophilic properties of methanol. Finally, the intermediate transforms directly to an ester product over Co–CoO@N-doped carbon using O_2 as an oxidant. In this sense, the catalyst can be used for both cross- and homo-coupling esterifications in only one procedure under mild conditions and the use of harmful oxidants is avoided.

In summary, a facile route has been developed to generate Co NPs with surface-oxidized CoO species uniformly incorporated in N-doped porous carbon by one-step pyrolysis of mono-dispersed and structurally well-organized MOF, ZIF-67, as a hard template. The approach effectively avoids the aggregation of incorporated high-density NPs. The resultant nanocomposites as inexpensive, stable and magnetically recyclable catalysts exhibit excellent catalytic performance for direct homo- and cross-coupling esterifications of primary alcohols under mild conditions, with 1 bar of O_2 as an environmentally friendly oxidant. The special structure of the nanocomposite and the synergistic effect between Co and CoO NPs are proposed to be responsible for the superior activity to other related catalysts. The N-doped porous carbon scaffold not only stabilizes the NPs but also greatly facilitates the accessibility and adsorption of substrates to the active sites and the diffusion of products. The current direct pyrolysis through the MOF-based template approach is facile and versatile and thus paves a way to diverse metal or metal oxide NPs thoroughly distributed porous carbon nanocomposites, which might find broad applications in many fields, especially in catalysis. A newly published study reporting similar results came to our attention during the proof stage.¹⁷

This work was supported by the NSFC (21371162 and 51301159), the 973 program (2014CB931803), the Recruitment Program of Global Youth Experts and the Fundamental Research Funds for the Central Universities (WK2060190026).

Notes and references

- (a) R. C. Larock, *Comprehensive Organic Transformations*, VCH, New York, 1989, p. 966; (b) J. Otera, *Esterification: Methods, Reaction and Applications*, Wiley-VCH, Weinheim, Germany, 2003.
- (a) C. Liu, J. Wang, L. Meng, Y. Deng, Y. Li and A. Lei, *Angew. Chem., Int. Ed.*, 2011, **50**, 5144; (b) R. L. Oliveira, P. K. Kiyohara and L. M. Rossi, *Green Chem.*, 2009, **11**, 1366; (c) C. Gunanathan, L. J. W. Shimon and D. Milstein, *J. Am. Chem. Soc.*, 2009, **131**, 3146; (d) M. Nielsen, H. Junge, A. Kammer and M. Beller, *Angew. Chem., Int. Ed.*, 2012, **51**, 5711; (e) T. Ishida, Y. Ogihara, H. Ohashi, T. Akita, T. Honma, H. Oji and M. Haruta, *ChemSusChem*, 2012, **5**, 2243; (f) P. Zhang, Y. Gong, H. Li, Z. Chen and Y. Wang, *Nat. Commun.*, 2013, **4**, 1593.
- (a) R. V. Jagadeesh, H. Junge, M.-M. Pohl, J. Radnik, A. Brückner and M. Beller, *J. Am. Chem. Soc.*, 2013, **135**, 10776; (b) R. Ray, R. D. Jana, M. Bhadra, D. Maiti and G. K. Lahiri, *Chem. – Eur. J.*, 2014, **20**, 15618.
- (a) J. R. Long and O. M. Yaghi, *Chem. Soc. Rev.*, 2009, **38**, 1213; (b) H.-C. Zhou and S. Kitagawa, *Chem. Soc. Rev.*, 2014, **43**, 5415.
- (a) J. Liu, P. K. Thallapally, B. P. McGrail, D. R. Brown and J. Liu, *Chem. Soc. Rev.*, 2012, **41**, 2308; (b) M. P. Suh, H. J. Park, T. K. Prasad and D.-W. Lim, *Chem. Rev.*, 2012, **112**, 782; (c) P. Nugent, S. Ma, M. Eddaoudi and M. J. Zaworotko, *et al.*, *Nature*, 2013, **495**, 80; (d) Y. He, W. Zhou, G. Qian and B. Chen, *Chem. Soc. Rev.*, 2014, **43**, 5657; (e) Z. Hu, K. Zhang, M. Zhang, Z. Guo, J. Jiang and D. Zhao, *ChemSusChem*, 2014, **7**, 2791; (f) F. Wang, H. Fu, Y. Kang and J. Zhang, *Chem. Commun.*, 2014, **50**, 12065.
- (a) D. Farrusseng, S. Aguado and C. Pinel, *Angew. Chem., Int. Ed.*, 2009, **48**, 7502; (b) A. Corma, H. García and F. X. Llabrés i Xamena, *Chem. Rev.*, 2010, **110**, 4606; (c) H.-L. Jiang and Q. Xu, *Chem. Commun.*, 2011, **47**, 3351; (d) J. Gascon, A. Corma, F. Kapteijn and F. X. Llabrés i Xamena, *ACS Catal.*, 2014, **4**, 361.
- (a) B. Chen, S. Xiang and G. Qian, *Acc. Chem. Res.*, 2010, **43**, 1115; (b) Y. Takashima, V. Martinez, S. Furukawa, M. Kondo, S. Shimomura, H. Uehara, M. Nakahama, K. Sugimoto and S. Kitagawa, *Nat. Commun.*, 2011, **2**, 168.
- (a) Z. Wang and S. M. Cohen, *Chem. Soc. Rev.*, 2009, **38**, 1315; (b) J. An, S. J. Geib and N. L. Rosi, *J. Am. Chem. Soc.*, 2009, **131**, 8376; (c) P. Horcajada, R. Gref, T. Baati, P. K. Allan, G. Maurin, P. Couvreur, G. Férey, R. E. Morris and C. Serre, *Chem. Rev.*, 2012, **112**, 1232.
- (a) H.-L. Jiang, B. Liu, Y.-Q. Lan, K. Kuratani, T. Akita, H. Shioyama, F. Zong and Q. Xu, *J. Am. Chem. Soc.*, 2011, **133**, 11854; (b) B. Liu, X. Zhang, H. Shioyama, T. Mukai, T. Sakai and Q. Xu, *J. Power Sources*, 2010, **195**, 857; (c) W. Cho, S. Park and M. Oh, *Chem. Commun.*, 2011, **47**, 4138; (d) X. Xu, R. Cao, S. Jeong and J. Cho, *Nano Lett.*, 2012, **12**, 4988; (e) M. Y. Masoomi and A. Morsali, *Coord. Chem. Rev.*, 2012, **256**, 2921; (f) N. L. Torad, M. Hu, S. Ishihara, H. Sukegawa, A. Belik, M. Imura, K. Ariga, Y. Sakka and Y. Yamauchi, *Small*, 2014, **10**, 2096; (g) Y. Lü, W. Zhan, Y. He, Y. Wang, X. Kong, Q. Kuang, Z. Xie and L. Zheng, *ACS Appl. Mater. Interfaces*, 2014, **6**, 4186; (h) T. K. Kim, K. J. Lee, J. Y. Cheon, J. H. Lee, S. H. Joo and H. R. Moon, *J. Am. Chem. Soc.*, 2013, **135**, 8940; (i) J.-K. Sun and Q. Xu, *Energy Environ. Sci.*, 2014, **7**, 2071; (j) H. Jin, J. Wang, D. Su, Z. Wei, Z. Pang and Y. Wang, *J. Am. Chem. Soc.*, 2015, **137**, 2688.
- (a) S. Ma, G. A. Goenaga, A. V. Call and D. Liu, *Chem. – Eur. J.*, 2011, **17**, 2063; (b) P. Zhang, F. Sun, Z. Xiang, Z. Shen, J. Yun and D. Cao, *Energy Environ. Sci.*, 2014, **7**, 442; (c) P. Su, H. Xiao, J. Zhao, Y. Yao, Z. Shao, C. Li and Q. Yang, *Chem. Sci.*, 2013, **4**, 2941; (d) W. Zhang, Z.-Y. Wu, H.-L. Jiang and S.-H. Yu, *J. Am. Chem. Soc.*, 2014, **136**, 14385; (e) S. Zhao, H. Yin, L. Du, L. He, K. Zhao, L. Chang, G. Yin, H. Zhao, S. Liu and Z. Tang, *ACS Nano*, 2014, **8**, 12660.
- (a) C. Bai, X. Yao and Y. Li, *ACS Catal.*, 2015, **5**, 884; (b) G. Yu, J. Sun, F. Muhammad, P. Wang and G. Zhu, *RSC Adv.*, 2014, **4**, 38804.
- (a) R. Banerjee, A. Phan, B. Wang, C. Knobler, H. Furukawa, M. O’Keeffe and O. M. Yaghi, *Science*, 2008, **319**, 939; (b) J. Qian, F. Sun and L. Qin, *Mater. Lett.*, 2012, **82**, 220.
- (a) M. C. Biesinger, B. P. Payne, A. P. Grosvenor, L. W. M. Lau, A. R. Gerson and R. St. C. Smart, *Appl. Surf. Sci.*, 2011, **257**, 2717; (b) J. Zhu, K. Kailasam, A. Fischer and A. Thomas, *ACS Catal.*, 2011, **1**, 342.
- S. Chen, J. Bi, Y. Zhao, L. Yang, C. Zhang, Y. Ma, Q. Wu, X. Wang and Z. Hu, *Adv. Mater.*, 2012, **24**, 5593.
- C. Tang, C. Wang and S.-H. Chien, *Thermochim. Acta*, 2008, **473**, 68.
- (a) P. Haide and A. Baiker, *J. Catal.*, 2007, **248**, 175; (b) F.-Z. Su, Y.-M. Liu, L.-C. Wang, Y. Cao, H.-Y. He and K.-N. Fan, *Angew. Chem., Int. Ed.*, 2008, **47**, 334.
- W. Zhong, H. Liu, C. Bai, S. Liao and Y. Li, *ACS Catal.*, 2015, **5**, 1850.